Application of Cu(II) and Zn(II) coproporphyrins as sensitizers for thin film dye sensitized solar cells

Leila Alibabaei,[ab] Mingkui Wang,[a] Rita Giovannetti,[b] Joël Teuscher,[a] Davide Di Censo,[a] Jacques-E. Moser,[a] Pascal Comte,[a] Filippo Pucciarelli,[b] Shaik M. Zakeeruddin*[a] and Michael Grätzel*[a]

Received 17th December 2009, Accepted 22nd March 2010
First published as an Advance Article on the web 24th May 2010
DOI: 10.1039/b926726c

We synthesized the Cu(II) and Zn(II) complexes of the 2,7,12,17-tetrapropionic acid of 3,8,13,18-tetramethyl-21*H*,23*H* porphyrin (coproporphyrin-I) and successfully employed them as sensitizers in dye-sensitized solar cells. Copper(II) coproporphyrin-I exhibits a power conversion efficiency of 3.8% measured under irradiation of AM 1.5G full sunlight (100 mW cm^{-2}).

1. Introduction

Dye-sensitized solar cells (DSC) have attracted considerable attention over the past decade as a viable alternate technology for renewable energy.[1] In the search of new sensitizers, recent improvements in the design and synthesis of new ruthenium dyes have made it possible to overcome the previously attained threshold of 11% light-to-energy conversion.[2] In view of the limited availability of ruthenium, much effort has been directed towards the development of noble metal-free sensitizers because of their lower cost, high molar extinction coefficient and easy to tune the spectral properties.[3–5]

The interest in using porphyrins as sensitizers in photovoltaic applications has recently intensified and has led to a better understanding of the key role of porphyrins found in the natural photosynthetic processes. In fact there are several analogies between natural photosynthesis and dye-sensitized PV devices employing nanocrystalline semiconductor electrodes; the efficient light harvesting witnessed in plants has been successfully imitated by absorbing a monolayer of the chlorophyll derivates on nanostructured TiO_2 films.[6,7] Previous studies on chlorophyll derivatives showed that conjugation with the π-electron system of the chromophore is not critical for efficient electron transfer, but that the insertion of free carboxylic groups is important for anchoring on the surface of TiO_2.[6,8,9] Numerous reports on porphyrin based DSCs have been published.[10–16]

The nature of the carboxylic acid linker on the porphyrin has a significant influence on the performance of the devices.[17] Mesoporphyrin IX is a free-base porphyrin that contains two carboxylic groups found at the β-position. When utilizing its Cu(II) and Zn(II) complexes as sensitizers in DSC, the energy conversion efficiency of the cell was reported to be ≅ 2.6%.[4] The study of Zn(II) and Cu(II) complexes of 4-(*trans*-2′-(2″-(5″,10″,15″,20″-tetraphenylporphyrinato-copper(II)yl)ethen-1′-yl)-1-benzoic acid, and 4-(*trans*-2′-(2″-(5″,10″,15″,20″-tetraxylylporphyrinato-zinc(II)yl)-ethen-1″-yl)-1-benzoic acid porphyrins that contain one carboxylic group in the β-position, have been undertaken. The highest conversion efficiencies were obtained when employing the Zn-porphyrin complexes, with a yield of 4.11 and 4.80%, respectively.[18] Moreover, with zinc tetraaryl porphyrin malonic acids, an efficiency of 7.10% was found.[19] Using SnO_2 as photoanode, the influence of the metal substitution on the photocurrent efficiency of carboxyphenyl metalloporphyrins, (containing one carboxylic group in *meso*-position) as photosensitizer has been studied by Otero *et al.*[20] In this manuscript, the 2,7,12,17-tetrapropionicacid of 3,8,13,18-tetramethyl-21*H*,23*H*-porphyrin (coproporphyrin-I or CPI) metal complexes of Cu(II) and Zn(II) (Fig. 1) have been synthesized and their use as sensitizers in DSC has been evaluated.

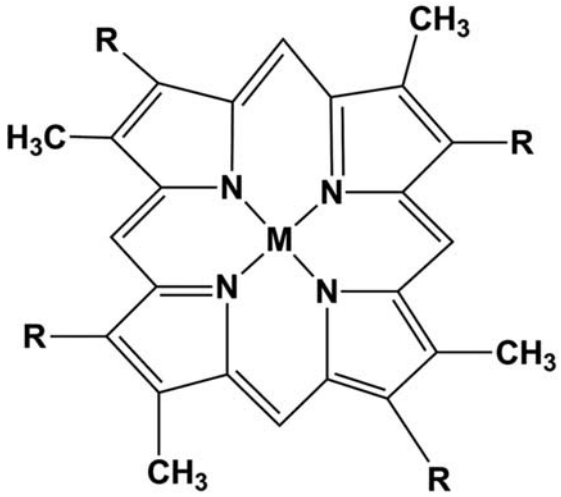

Fig. 1 Molecular structures of Coproporphyrin-I sensitizers, R = -CH_2CH_2COOH; CPI = M is no metal, CPIZn = M is Zn(II), CPICu = M is Cu(II).

2. Experimental

2.1 Reagents

CPI-dihydrochloride, $ZnCl_2$ and $CuCl_2$ are analytical grade reagent obtained from Sigma-Aldrich. Ethanol, analytical grade,

[a]*Laboratory for Photonics and Interfaces, Ecole Polytechnique Fédérale de Lausanne, CH 1015 Lausanne, Switzerland. E-mail: shaik.zakeer@epfl.ch; michael.graetzel@epfl.ch*
[b]*Chemistry Section of Department of Environmental Science, University of Camerino, Via S.Agostino,1, 62032 Camerino, MC, Italy*

and 1-ethyl-3-methylimidazolium tetracyanoborate ($EMI^+B(CN)_4^-$) were purchased from Fluka and Merck, respectively.

2.2 Synthesis and characterization

2.2.1 Synthesis of CPIZn. CPI dihydrochloride (96 mg, 132 mM) was dissolved in 200 ml of ethanol solution and mixed with 6 ml zinc chloride (19 mg, 139 mM) under nitrogen atmosphere, and the mixture stirred for 3 h at room temperature. The solvent was then evaporated under vacuum, and the residue dried under nitrogen atmosphere. The compound obtained was dissolved in 40 ml ethanol and precipitated following the addition of 100 ml water. The solid compound was collected by filtration and washed with 200 ml water. This procedure was repeated four times. and the pink solid was collected and dried under nitrogen atmosphere. Elemental analysis: calc. (%) for $C_{36}H_{36}N_4O_8Zn \cdot H_2O$: C, 58.7; H, 5.2; N, 7.6; found: C, 59.0; H, 5.5; N, 7.2. ^{1}H NMR (400 MHz, DMSO, 45 °C): δ 12.28 (s, 4H); 10.27 (s, 4H), 4.37–4.29 (t, 8H), 3.17–3.13 (t, 8H). ESI-Mass: MS (API-ES): (M = 718,04) neg, (m/z): 717, 653.4, 479.4, 357.1, 293.2.

2.2.2 Synthesis of CPICu. The copper coproporphyrin complex was synthesized following the same procedure as outlined above by replacing zinc(II) chloride by copper(II) chloride. Elemental analysis: calc. (%) for $C_{36}H_{36}N_4O_8Cu \cdot H_2O$: C, 58.9; H, 5.2; N, 7.6; found: C, 58.9; H, 5.5; N: 7.2. ^{1}H NMR (400 MHz, DMSO, 45 °C): δ 12.231 (s, 4H); 10.21 (s, 4 H), 4.36–4.28 (t, 8H), 3.21–3.41 (t, 8H). ESI-Mass: MS (API-ES) (M = 716), neg, (m/z): 715, 476.7, 367.7, 356.6, 237.6

2.2.3 Characterization. The UV-visible absorption spectra were recorded on a Hewlett- Packard 8452A diode array spectrophotometer employing a 1 cm quartz cell connected to a Lauda K2R thermostat, by monitoring the spectral change against a blank, at constant temperature (20 °C). Cyclic voltammetry experiments were performed using a computer-controlled EG&G PAR 273 potentiostat in a three-electrode single-compartment cell with a platinum working electrode, a platinum wire counter electrode, and an Ag/AgCl reference electrode. All potentials were internally referenced to the ferrocene–ferrocenium couple.

2.3 Device fabrication and characterization:

2.3.1 Device fabrication. Screen-printed double layers of TiO_2 particles were used as photoelectrodes in this study. A 7.5 μm thick film of 20 nm-sized TiO_2 particles was first printed on the fluorine doped SnO_2 (FTO) conducting glass electrode and coated with a second layer (5 μm thick) composed of 400 nm light-scattering anatase particles (CCI, Japan). The porosity was evaluated as 67% for the 20 nm TiO_2 transparent layer and 42% for the 400 nm TiO_2 scattering layer, determined from BET measurements. After sintering at 500 °C and cooling to 80 °C, the sintered TiO_2 electrodes were immersed for 5 h in the respective dye solutions (0.3 mM in 10% DMSO and ethanol with chenodeoxycholic acid (2 mM) as a co-adsorbent), and then assembled using a thermal platinized FTO/glass counter electrode. The working and counter electrodes were separated by a 25 μm thick hot melt ring (Surlyn, DuPont) and sealed by heating. The cell's internal space was filled with appropriate electrolyte using a vacuum pump. The hole for electrolyte-injection on the thermally platinized FTO glass counter electrode was finally sealed with a Surlyn sheet and a thin glass cover by heating.

2.3.2 Photovoltaic characterization. A 450 W xenon light source (Oriel, USA) was used to characterize the solar cells. The spectral output of the lamp was matched in the region of 350–750 nm with the aid of a Schott K113 Tempax sunlight filter (Präzisions Glas & Optik GmbH, Germany) so as to reduce the mismatch between the simulated and true solar spectra to less than 2%. The current–voltage characteristics of the cell under these conditions were obtained by applying an external potential bias to the cell and measuring the generated photocurrent with a Keithley model 2400 digital source meter (Keithley, USA). A similar data acquisition system was used to control the incident photon-to-current conversion efficiency (IPCE) measurement. Under computer control, light from a 300 W xenon lamp (ILC Technology, USA) was focused through a Gemini-180 double monochromator (Jobin Yvon Ltd., UK) onto the photovoltaic cell under test. The devices were masked to attain an illuminated active area of 0.158 cm^2.

2.3.3 Laser study. The nanosecond laser flash photolysis technique was applied to dye-sensitized, 8 μm-thick, transparent TiO_2 mesoporous films deposited on normal flint glass. Pulsed excitation (λ = 532 nm, 7 ns pulse duration, 30 Hz repetition rate) was carried out by a Powerlite 7030 frequency-doubled Q–switched Nd:YAG laser (Continuum, Santa Clara, California, USA). The laser beam output was expanded by a planoconcave lens to irradiate a large cross-section of the sample, whose surface was kept at a 30° angle to the excitation beam. The laser fluence on the sample was kept at a low level (30 μJ cm^{-2} per pulse) to ensure that, on average, less than one electron is injected per nanocrystalline TiO_2 particle on pulsed irradiation. The probe light, produced by a continuous wave xenon arc lamp, was first passed through a monochromator tuned at 650 nm, various optical elements, the sample, and then through a second monochromator, before being detected by a fast photomultiplier tube (Hamamatsu, R9110). Data waves were recorded on a DSA 602A digital signal analyser (Tektronix, Beaverton, Oregon, USA). Satisfactory signal-to-noise ratios were typically obtained by averaging over 1500 laser shots.

2.3.4 Transient photoelectrical measurements. Transient photovoltage and photocurrent decay characteristics were measured using methodology developed in our group.[21,22] In the transient photovoltage decay experiments, different steady-state light levels were supplied with a home-made white light-emitting diode array by tuning the driving voltage. A red light-emitting diode array controlled with a fast solid-state switch was used to generate a perturbation pulse with a width of 50 ms. Both the pulsed red- and steady-state white-lights were both incident on the photoanode side of the cell being tested. The pulsed red lights were carefully controlled by utilizing the driving potential of the red diode array to keep the modulated photovoltage below 10 mV. The red light generated carriers causing a small photovoltage increase near the V_{oc} of the cell subjected to the white

bias light and the voltage decay process was thereafter measured. Normally, the decay follows closely a monoexponential form, thus the recombination rate constant can be extracted from the slope of the semi-logarithmic plot. The capacitance of the TiO_2/electrolyte interface and density of states (DOS) at the V_{oc} are calculated as $C_\mu = \Delta Q/\Delta V$, where ΔV is the peak of the photovoltage transient and ΔQ is the number of electrons injected during the red light flash. The latter is obtained by integrating a short-circuit photocurrent transient generated from an identical red-light pulse. Electron densities in the titania film under the same given white light intensity were determined by a charge extraction method, in which the light intensity was switched off completely, and simultaneously the solar cell was switched from open circuit to short circuit. The resulting current was integrated and based on the amount of extracted charge the electron density was calculated.

Table 1 Optical and electrochemical data of coproporphyrin-I sensitizers

Dye	Solvent	λ/nm (ϵ/L mol^{-1} cm^{-1})	$E^0_{ox}{}^a$/V	$E^0_{Red}{}^a$/V
CPI	Ethanol	396 (1.62×10^5) 496 (1.32×10^4) 530 (9.17×10^3) 568 (5.7×10^3) 620 (4.2×10^3)	0.52	− 1.81
CPIZn	10% DMSO–ethanol	408 (2.26×10^5) 538 (1.46×10^4) 574 (1.42×10^4)	0.18	− 2.01
CPICu	10% DMSO–ethanol	396 (2.16×10^5) 524 (1.21×10^4) 560 (2.23×10^4)	0.32	− 1.89

[a] Measured by cyclic voltammetry in DMF using 0.1 M tetrabutylammonium hexafluorophosphate as a supporting electrolyte scan rate = 100 mV s^{-1}, *vs.* Fc$^+$/Fc.

3. Results and discussion

The absorption spectra of these compounds are shown in Fig. 2. All coproporphyrin-I dyes used in this work exhibit maxima attributed to π–π* transitions in the range 350–450 nm for the Soret band and 500–650 nm for the Q bands. The molar extinction coefficients for the Soret band of these coproporphyrin-I dyes lie in the range (1.6–2.3) × 10^5 dm^3 mol^{-1} cm^{-1}, whereas those of the Q(0,0) band are in the range (4.2–14.6) × 10^3 dm^3 mol^{-1} cm^{-1}. Both the Soret and Q bands for CPIZn and CPICu show oscillator strengths comparable with that of CPI, with red shift in the absorption spectra due to the influence of metal ions (Table 1).

We employed cyclic voltammetry to determine the oxidation and reduction potentials of these coproporphyrins; the electrochemical reactions of these compounds were measured under ambient conditions. The electrochemical data are summarized in Table 1. All coproporphyrin-I dyes exhibit reversible waves for the oxidation, corresponding to the HOMO energy of the dye, at a potential greater than that of I^-/I_3^- couple, which assures regeneration of the neutral dye from its oxidized state. A reversible oxidation reaction was observed at $E_{1/2}$ = +0.52 V corresponding to the formation of $[CPI]^+$ whereas an irreversible reduction wave was observed at about E_{pc} = −1.81 V. For example, the oxidation occurs at +0.52 V for CPI, shifts to +0.32 V for CPICu, and further shifts to +0.18 V for CPIZn, whereas the reduction potential occurs at E_{pc} = −1.81 V for CPI and in a small range of −1.89 to −2.01 V for CPICu and CPIZn. The oxidation potential of CPIZn and CPICu is lower than CPI showing that the presence of metal ion influences the electron density at the CPI core structure (Table 1). Incorporation of metal ion onto the porphyrin ring decreases the electrochemical HOMO–LUMO energy gap, consistent with red shifts of both Soret and Q bands in the absorption spectra.

The *I–V* characteristic curve of the solar cell under illumination with standard AM 1.5G simulated sunlight (100 mW cm^{-2}) is displayed in Fig. 3. The CPICu-sensitized cell (device C) provides a J_{sc} of 7.8 mA cm^{-2}, a V_{oc} of 0.636 V and a fill factor

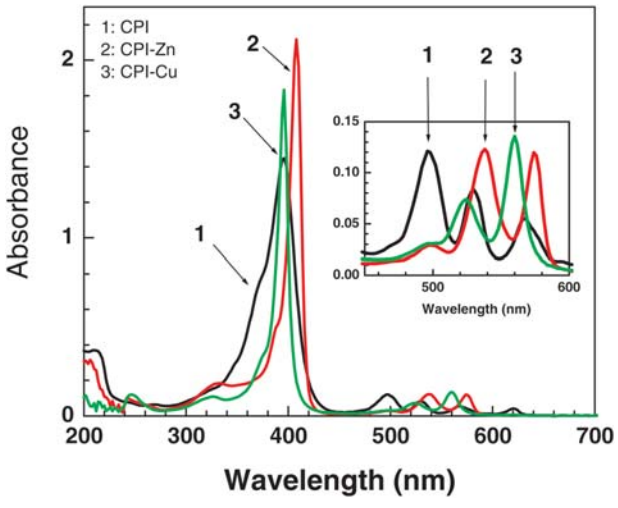

Fig. 2 Electronic absorption spectra of CPI measured in ethanol and CPIZn, CPICu in 10% DMSO–ethanol mixture.

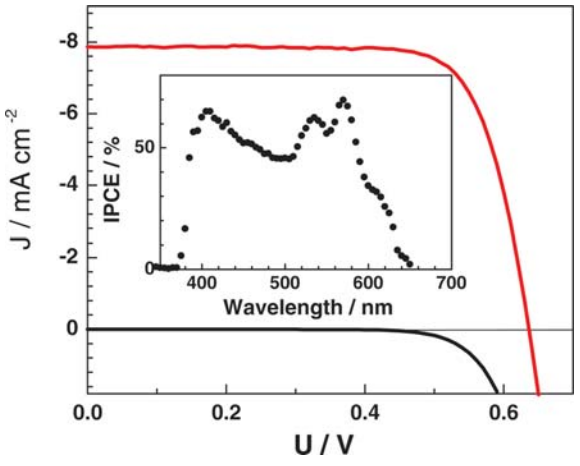

Fig. 3 Photocurrent density–voltage (*J–V*) characteristics of device C (Table 2) using CPICu as a sensitizer under AM 1.5G illumination (100 mW cm^{-2}). Double layer 7.5 μm + 5 μm TiO_2 film. Electrolyte Z960 composition: 1,3-dimethylimidazolium iodide = 1.0 M, iodine = 0.03 M, *tert*-butylpyridine = 0.5 M, LiI = 0.05 M, guanidinium thiocyanate = 0.1 M, in acetonitrile–valeronitrile mixture (85 : 15 v/v). Cells were tested using a metal mask with an aperture area of 0.158 cm^2. Inset is the incident photon to current conversion efficiency of the same device.

Table 2 Detailed photovoltaic parameters of DSCs made with coproporphyrins-I and Z960 electrolyte using TiO_2 films with two different thicknesses

Device	Dye	Film thickness/μm	V_{oc}/mV	J_{sc}/mA cm^{-2}	FF	Eff. (%)
A	CPI	7.5 + 5	490	2.55	0.74	0.9
B	CPIZn	7.5 + 5	565	6.0	0.75	2.6
C	CPICu	7.5 + 5	636	7.9	0.75	3.8
D	CPICu	3.3	655	5.7	0.70	2.6
E	CPIZn	3.3	504	3.17	0.72	1.1

(FF) of 0.75, yielding an overall power conversion efficiency of 3.8%. The thin-film (3.3 um) device D based on CPICu with the same electrolyte provides a J_{sc} of 5.7 mA cm^{-2}, a V_{oc} of 0.655 V and a FF of 0.695, yielding an overall conversion efficiency of 2.6% under illumination with AM 1.5G simulated sunlight (100 mW cm^{-2}). The open-circuit photovoltage of a DSC decreases with increasing film thickness, since an increase in the surface area enhances the undesired dark current. Fig. 3 inset shows the incident photon to current conversion efficiency (IPCE) of a CPICu device in the presence of the volatile electrolyte (Z960), which exhibits a broad range of absorption from 400 to 675 nm with a peak maximum of 70% at 575 nm. Table 2 summarizes the photovoltaic parameters for devices made with the three different coproporphyrins using volatile electrolyte Z960. The overall power conversion efficiencies vary as a function of the metal ion. First, CPIZn shows a cell performance much better than for our reference cell, CPI. Secondly, the substitution of zinc with copper, in the CPICu containing device, showed higher V_{oc} and J_{sc} values than that of CPIZn to obtain 3.8% efficiency.

Nanosecond time-resolved laser experiments were performed to elucidate the dye cation dynamics of interception by iodide (Fig. 4). The pulsed laser intensity was kept at a low level ($\leq$ 30 μJ cm^{-2} per pulse) so as to ensure that, on average, less than one S^+/e^- charge-separated sensitizer–electron pair was produced per nanocrystalline particle upon pulsed irradiation.

Ultrafast electron injection into the conduction band of TiO_2 (reaction (1), Scheme 1) is followed by a positive transient

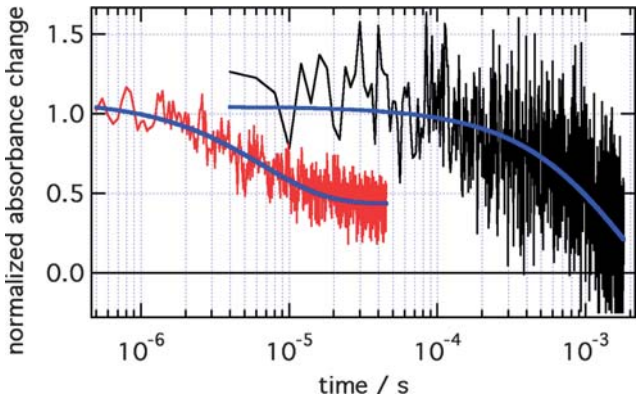

Fig. 4 Transient absorbance decay of the oxidized state of coproporphyrin-I sensitizers adsorbed on nanocrystalline TiO_2 films. The kinetics observed with acetonitrile, no iodide added (black curve), and in the presence of electrolyte Z960 (red/grey curve) under similar conditions.

$$S|TiO_2 + h\nu \rightarrow S^*|TiO_2 \rightarrow S^+|TiO_2 + e^-_{cb} \quad (1)$$
$$S^+|TiO_2 + e^-_{cb} \rightarrow S|TiO_2 \quad (2)$$
$$S^+|TiO_2 + 2I^- \rightarrow S|TiO_2 + I_2^{\bullet -} \quad (3)$$

Scheme 1

absorbance change that was observable at λ = 650 nm corresponding to absorption by oxidized coproporphyrin-I sensitizer. This positive transient permitted direct monitoring of the concentration of the oxidized state of the coproporphyrin-I sensitizers. In the absence of redox electrolyte, in pure acetonitrile, the decay of the transient absorbance reflected the dynamics of the recombination of conduction band electrons with the oxidized dye S^+ (reaction (2), Scheme 1). For the three coproporphyrins studied, decays were well fitted by monoexponential curves with τ = 673 μs, 1.03 ms and 1.8 ms for free base CPI, CPIZn and CPICu, respectively.

In the presence of acetonitrile based redox electrolyte (Z960), monitoring the transient at λ = 650 nm thus permitted monitoring of the dye cation interception by iodide. The decay of the oxidized dyes were markedly accelerated under these conditions. Monoexponential functions fitted the decays with τ = 23 μs, 7.7 μs and 6.7 μs for devices A, B and C, respectively. These results indicate that the sensitizer is quickly regenerated, the dye cation being efficiently intercepted by the redox mediator (reaction (3) in Scheme 1). Insertion of the metal ions into the CPI base enhances the dye regeneration process by a factor of 2.9 for zinc(II) ion, and 3.4 for copper(II) ion. Surprisingly for the three compounds, we observed the absorbance transient to reach a pseudo-plateau at approximately 30% of the initial signal magnitude. This residual absorbance, eventually decays down to the baseline within hundreds of μs, as observed for the recombination process in the absence of redox electrolyte, The origin of this residual absorption remains to be assigned.

By comparing monoexponential rate constants reported for the interception and recombination reactions, one is able to calculate the yield of interception by iodide.[23] The values thus obtained are 96.7, 99.3 and 99.6% for CPI, CPIZn and CPICu, respectively. Despite this large kinetic redundancy, a fraction of the dye cation is not fully intercepted by the electrolyte. Therefore, this could be one of the reasons for the low performance of the devices prepared with these three dyes, as 30% of the injected electrons might be lost due to recombination with the oxidized form of the dye.

Unraveling of the details of the electron recombination dynamics between the photoinjected electrons at the TiO_2 and the oxidized electrolyte in various devices was undertaken by employing transient photovoltage and photocurrent decay measurements. As presented in Fig. 5a, the chemical capacity C_μ of devices D and E rise exponentially with the increase of V_{oc}. As the density of states (DOS), including surface and bulk traps, is proportional to C_μ ($C_\mu \approx e^2 g(E)$, where e is electron charge, $g(E)$ is the DOS distribution function[21]), an exponential distribution of DOS could be obtained. As shown in Fig. 5a, the device E has a larger chemical capacitance than that of device D. Hence for both devices utilizing the same TiO_2 film thickness (3.3 μm), a higher trap states density is found in device E at a given V_{oc}. The chemical capacitance of device C increases as a function of the film thickness because a geometric area was used. Fig. 5b

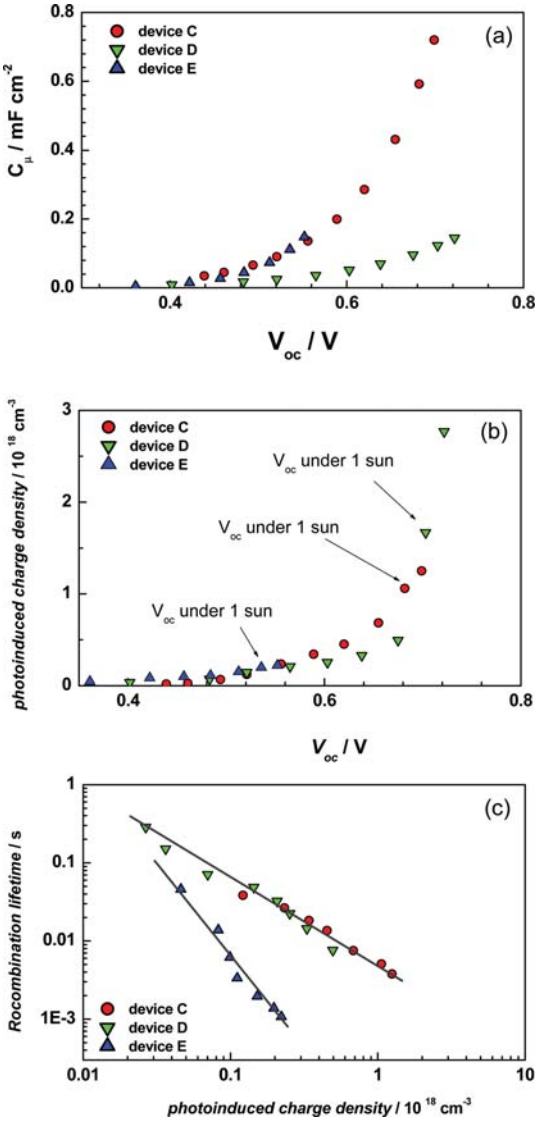

Fig. 5 (a) Chemical capacitance as a function of open circuit voltage, (b) photo-induced charge as a function of open circuit voltage, and (c) apparent electron lifetime with extracted charge obtained from transient voltage decay measurements. Device C was fabricated using a double layer (7.5 + 5 μm) TiO_2 film, a volatile electrolyte and using CPICu as a sensitizer. Devices D and E were fabricated using a 3.3 μm TiO_2 film, a volatile electrolyte and using CPICu and CPIZn as sensitizers, respectively.

illustrates the extracted charge density *vs*. open circuit voltage plot for various DSCs. As shown in Fig. 5b, for DSC devices sensitized with CPICu and CPIZn, the experimental points merge almost into the same curve. Note, as indicated on the figure, that the cells have different V_{oc} when illuminated at 1 sun as expected from the results illustrated before. The differences in voltage between the three devices may be due to: (a) a shift on the TiO_2 conduction band with respect to the electrolyte potential or (b) differences in the e_{cb}^-/mediator$^+$ recombination rate. In our case, the change of metal center does not shift the curve, thus, the differences in voltage could be due to the increase in the e_{cb}^-/mediator$^+$ recombination reaction rate in device E. Fig. 5c shows the recombination lifetime for various devices. It is noted that as the extracted charge density from the TiO_2 film increases, the recombination lifetimes (τ_e) are shortened, due to the higher electron density at the TiO_2 and larger driving forces for the interfacial recombination. Clearly, the trend of the charge recombination lifetime of the various devices is well in agreement with that of the above measured photocurrent densities. The recombination lifetime of the CPICu devices (C and D in Fig. 5c) employing two different film thicknesses exhibits only minor differences, showing an almost complete independence with respect to the film thickness. The device E shows the shortest recombination lifetime at a given extracted charge density, which is consistent with the photovoltaic performance.

Conclusion

In conclusion, we have synthesized two metal coproporphyrins-I containing Zn(II) and Cu(II) metal ions and successfully employed them as sensitizers in dye-sensitized solar cell. The photovoltaic performance of the Cu(II) coproporphyrin out performs that of the free base and the Zn(II) coproporphyrin. Now we are searching for new concepts to enhance the performance of dye-sensitized solar cells using metal porphyrins as sensitizers.

Acknowledgements

The authors thank Dr C. Grätzel and Prof. Vito Bartocci for fruitful discussions. Financial support from the Swiss National Science Foundation is gratefully acknowledged.

Notes and references

1 M. Grätzel, *Nature*, 2001, **414**, 338.
2 (*a*) M. Nazeeruddin, F. De Angelis, S. Fantacci, A. Selloni, G. Viscardi, P. Liska, S. Ito, B. Takeru and M. Grätzel, *J. Am. Chem. Soc.*, 2005, **127**, 16835; (*b*) Y. Chiba, A. Islam, Y. Watanabe, R. Komiya, N. Koide and L. Han, *Jpn. J. Appl. Phys.*, 2006, **45**, L638; (*c*) F. Gao, Y. Wang, D. Shi, J. Zhang, M. Wang, X. Jing, R. Humphry-Baker, P. M. Wang, S. Zakeeruddin and M. Grätzel, *J. Am. Chem. Soc.*, 2008, **130**, 10720; (*d*) C. Chen, M. Wang, J. Li, N. Pootrakulchote, L. Alibabaei, C. Ngoc-le, J.-D. Decoppet, J. H. Tsai, C. Grätzel, C.-G. Wu, S. M. Zakeeruddin and M. Grätzel, *ACS Nano*, 2009, **3**, 3103.
3 (*a*) K. Hara, K. Sayama, Y. Ohga, A. Shinpo, S. Suga and H. Arakawa, *Chem. Commun.*, 2001, 569; (*b*) K. Hara, M. Kurashige, S. Ito, A. Shinpo, S. Suga, K. Sayama and H. Arakawa, *Chem. Commun.*, 2003, 252; (*c*) K. Hara, M. Kurashige, Y. Danoh, C. Kasada, A. Shinpo, S. Suga, K. Sayama and H. Arakawa, *New J. Chem.*, 2003, **27**, 783; (*d*) Z.-S. Wang, Y. Cui, Y. Dan-oh, C. Kasada, A. Shinpo and K. Hara, *J. Phys. Chem. C*, 2007, **111**, 7224; (*e*) T. Horiuchi, H. Miura and S. Uchida, *Chem. Commun.*, 2003, 3036; (*f*) T. Horiuchi, H. Miura, K. Sumioka and S. Uchida, *J. Am. Chem. Soc.*, 2004, **126**, 12218; (*g*) T. Kitamura, M. Ikeda, K. Shigaki, T. Inoue, N. A. Anderson, X. Ai, T. Lian and S. Yanagida, *Chem. Mater.*, 2004, **16**, 1806; (*h*) K. Hara, T. Sato, R. Katoh, A. Furabe, T. Yoshihara, M. Murai, M. Kurashige, S. Ito, A. Shinpo, S. Suga and H. Arakawa, *Adv. Funct. Mater.*, 2005, **15**, 246; (*i*) S. Kim, H. Choi, D. Kim, K. Song, S. O. Kang and J. Ko, *Tetrahedron*, 2007, **63**, 9206; (*j*) S. Kim, H. Choi, C. Baik, K. Song, S. O. Kang and J. Ko, *Tetrahedron*, 2007, **63**, 11436.
4 (*a*) Z.-S. Wang, Y. Cui, K. Hara, Y. Dan-ho, C. Kasada and A. Shinpo, *Adv. Mater.*, 2007, **19**, 1138; (*b*) A. Mishra, M. K. R. Fischer and P. Bäuerle, *Angew. Chem., Int. Ed.*, 2009, **48**, 2474; (*c*) I. Jung, J. K. Lee, K. H. Song, K. Song, S. O. Kang and J. Ko, *J. Org. Chem.*, 2007, **72**, 3652; (*d*) M. Velusamy, K. R. J. Thomas, J. T. Lin, Y. Hsu and K. Ho, *Org. Lett.*, 2005, **7**,

1899; (*e*) D. P. Hagberg, T. Edvinsson, T. Marinado, G. Boschloo, A. Hagfeldt and L. Sun, *Chem. Commun.*, 2006, 2245; (*f*) S. Ferrere, A. Zaban and B. A. Greg, *J. Phys. Chem. B*, 1997, **101**, 4490; (*g*) S. Ferrere and B. A. Greg, *New J. Chem.*, 2002, **26**, 1155; (*h*) Y. Shibano, T. Umeyama, Y. Matano and H. Imahori, *Org. Lett.*, 2007, **9**, 1971; (*i*) A. Ehret, L. Stuhl and M. T. Spitler, *J. Phys. Chem. B*, 2001, **105**, 9960; (*j*) S. Ushiroda, N. Ruzycki, Y. Lu, M. T. Spitler and B. A. Parkinson, *J. Am. Chem. Soc.*, 2005, **127**, 5158.

5 (*a*) S. Ito, S. M. Zakeeruddin, R. Humphry-Baker, P. Liska, R. Charvet, P. Comte, M. K. Nazeeruddin, P. Péchy, M. Takata, H. Miura, S. Uchida and M. Grätzel, *Adv. Mater.*, 2006, **18**, 1202; (*b*) M. Liang, W. Xu, F. Cai, P. Chen, B. Peng, J. Chen and Z. Li, *J. Phys. Chem. C*, 2007, **111**, 4465; (*c*) S. Tatay, S. A. Haque, B. O'Regan, J. R. Durrant, W. J. H. Verhees, J. M. Kroon, A. Vidal- Ferran, P. Gaviña and E. Palomares, *J. Mater. Chem.*, 2007, **17**, 3037; (*d*) Q.-H. Yao, L. Shan, F.-Y. Li, D.-D. Yin and C. H. Huang, *New J. Chem.*, 2003, **27**, 1277; (*e*) Y.-S. Chen, C. Li, Z.-H. Zeng, W.-B. Wang, X.-S. Wang and B.-W. Zhang, *J. Mater. Chem.*, 2005, **15**, 1654.

6 A. Kay and M. Grätzel, *J. Phys. Chem.*, 1993, **97**, 6272.

7 L. Otero, H. Osora, W. Li and M. A. Fox, *J. Porphyrins Phthalocyanines*, 1998, **2**, 123.

8 K. Kalyanasundaram and M. Grätzel, *Coord. Chem. Rev.*, 1998, **177**, 347.

9 A. Kay, R. Humphry-Baker and M. Grätzel, *J. Phys. Chem.*, 1994, **98**, 952.

10 (*a*) W. M. Campbell, A. K. Burrell, D. L. Officer and K. W. Jolley, *Coord. Chem. Rev.*, 2004, **248**, 1363; (*b*) C.-W. Lee, H.-P. Lu, C.-M. Lan, Y.-L. Huang, Y.-R. Liang, W.-N. Yen, Y.-C. Liu, Y.-S. Lin, E. W.-G. Diau and C.-Y. Yeh, *Chem.–Eur. J.*, 2009, **15**, 1403; (*c*) H.-P. Lu, C.-L. Mai, C.-Y. Tsia, S.-j. Hsu, C.-P. Hsieh, C.-L. Chiu, C.-Y. Yeh and E. W.-G. Diau, *PhysChemPhys*, 2009, **11**, 10270.

11 R. Dabestani, A. J. Bard, A. Campion, M. A. Fox, T. E. Mallouk, S. E. Webber and J. M. White, *J. Phys. Chem.*, 1988, **92**, 1872.

12 G. K. Boschloo and A. Goossens, *J. Phys. Chem.*, 1996, **100**, 19489.

13 C. C. Wamser, H.-S. Kim and J.-K. Lee, *Opt. Mater.*, 2003, **21**, 221.

14 S. Cherian and C. C. Wamser, *J. Phys. Chem.*, 2000, **104**, 3624.

15 H. Imahori, T. Umeyama and S. Ito, *Acc. Chem. Res.*, 2009, **42**, 1809.

16 T. Ma, K. Inoue, K. Yao, H. Noma, T. Shuji, E. Abe, J. Yu, J. Wang and B. Zhang, *J. Electroanal. Chem.*, 2002, **537**, 31.

17 Q. Wang, W. M. Campbell, E. E. Bonfantani, K. W. Jolley, D. L. Officer, P. J. Walsh, K. Gordon, R. Humphry-Baker, M. K. Nazeeruddin, and M. Grätzel, *J. Phys. Chem. B*, 2005, **109**, 15397.

18 Md. K. Nazeeruddin, R. Humphry-Baker, D. L. Officer, W. M. Campbell, A. K. Burrell and M. Grätzel, *Langmuir*, 2004, **20**, 6514.

19 W. M. Campbell, K. W. Jolley, P. Wagner, K. Wagner, P. J. Walsh, K. C. Gordon, L. Schmidt-Mende, M. K. Nazeeruddin, Q. Wang, M. Grätzel and D. L. Officer, *J. Phys. Chem. Lett.*, 2007, **111**, 11760.

20 M. Gervaldo, F. Fungo, E. N. Durantini, J. J. Silber, L. Sereno and L. Otero, *J. Phys. Chem. B*, 2005, **109**, 20953.

21 M. Wang, P. Chen, R. Humphry-Baker, S. M. Zakeeruddin and M. Grätzel, *ChemPhysChem*, 2009, **10**, 290.

22 M. Wang, C. Grätzel, S. J. Moon, R. Humphry-Baker, N. Rossier-Iten, S. M. Zakeeruddin and M. Grätzel, *Adv. Funct. Mater.*, 2009, **19**, 2163.

23 Z. Zhang, S. Ito, J.-E. Moser, S. M. Zakeeruddin and M. Grätzel, *ChemPhysChem*, 2009, **10**, 1834.